RADIAL VELOCITY PROPERTIES OF BINARY CEMP-R/S STARS

An Undergraduate Research Scholars Thesis

by

JARED LEE CATHEY

Submitted to the LAUNCH: Undergraduate Research office at
Texas A&M University
in partial fulfillment of the requirements for the designation as an

UNDERGRADUATE RESEARCH SCHOLAR

Approved by
Faculty Research Advisor: Jennifer L.Marshall

May 2021

Major: Physics[1]

RESEARCH COMPLIANCE CERTIFICATION

Research activities involving the use of human subjects, vertebrate animals, and/or biohazards must be reviewed and approved by the appropriate Texas A&M University regulatory research committee (i.e., IRB, IACUC, IBC) before the activity can commence. This requirement applies to activities conducted at Texas A&M and to activities conducted at non-Texas A&M facilities or institutions. In both cases, students are responsible for working with the relevant Texas A&M research compliance program to ensure and document that all Texas A&M compliance obligations are met before the study begins.

I, Jared Lee Cathey[1], certify that all research compliance requirements related to this Undergraduate Research Scholars thesis have been addressed with my Research Faculty Advisor prior to the collection of any data used in this final thesis submission.

This project did not require approval from the Texas A&M University Research Compliance & Biosafety office.

TABLE OF CONTENTS

ABSTRACT

Radial Velocity Properties of Binary CEMP-r/s Stars

Jared Lee Cathey[1]
Department of Physics and Astronomy[1]
Texas A&M University

Research Faculty Advisor: Jennifer L. Marshall
Department of Physics and Astronomy
Texas A&M University

Low metallicity stars allow us to better understand the chemical evolution of the Milky Way. A large fraction of low metallicity stars show large enhancements in carbon. These stars are known as Carbon Enhanced Metal Poor stars (CEMP stars). A subgroup of these show enhancements of neutron-capture elements through both the slow (s) and rapid (r) neutron-capture processes, these stars are called CEMP-r/s stars. How these stars get their peculiar abundance patterns is currently unknown, but in similar types of stars it has been shown that mass transfer in binary systems plays a significant role in their abundance patterns. If binaries do play a significant role in the enhancement of CEMP-r/s stars, I expect to find a large fraction of the stars I am studying to be in binary systems. The goal of this project is to better understand what role binaries have in the formation and enrichment of CEMP-r/s stars. I have been analyzed optical spectra obtained over the past two years for a sample of CEMP-r/s stars by Dr. Terese T. Hansen at the McDonald Observatory. Using the astronomical image reduction software IRAF I have extracted radial velocity data to combine with literature data and use this to identify possible binary systems. The results of this appear to show a strong correlation between CEMP-r/s stars being in binary systems, with an optimistic estimate of 85.7% of CEMP-r/s stars in this data may be binaries.

ACKNOWLEDGMENTS

Contributors

I would like to thank my faculty advisor, Dr. Jennifer Marshall, for her guidance and support throughout the course of this research.

Thanks also go to my friends and colleagues and the department faculty and staff for making my time at Texas A&M University a great experience.

The data analyzed for Radial Velocity Properties of Binary CEMP-r/s Stars were provided by Dr. Terese T. Hansen who also played a major role in my guidance throughout this research, and I would also like to thank her as well.

All other work conducted for the thesis was completed by the student independently.

Funding Sources

This project did not receive any funding. This paper includes data taken at The McDonald Observatory of The University of Texas at Austin.

1. INTRODUCTION

1.1 Galactic Chemical Evolution

As the Milky Way has evolved, it is widely accepted that the average metallicities of stars in it has been increasing. This is because in the early universe stars would have all been composed of almost entirely hydrogen. This hydrogen, alongside helium and trace amounts of heavier elements, were the only elements available at this early stage of the universe. These stars are referred to as Population III stars and are believed to be the first generation of stars. It is believed that these Population III stars then went through their evolution and began to enrich the surrounding region through supernovae with heavier elements [1]. Following this, the newly created heavier elements then seeded the gas clouds which would go on to collapse into new, more metal rich, stars which would then go on to similarly seed future generations. As galaxies formed, they were populated by further enriched stars leading to the aforementioned increasing metallicity trend. Because of this, we can infer that stars in our own Milky Way with lower metallicities are likely older, as oppose to newer stars which will have higher metallicities on average.

The processes by which stars are enriched with different elements will correspond with different astrophysical phenomena. The deaths of Population III stars would have seeded their surrounding region with elements through to Iron [1]. The second generation of stars which are seeded by this are then able to create elements heavier than iron through multiple processes. The first I will discuss is the slow neutron-capture process (s-process). It is widely believed that the s-process occurs primarily in asymptotic giant branch (AGB) stars [2], which is a stage in the stellar evolution of lower mass stars, $0.6 - 10 M_{\odot}$, after they have left the main sequence. This s-process will produce elements heavier than iron such as Strontium, Barium, and Lead. Another process that created many of the elements would be the rapid neutron-capture process (r-process). The r-process creates many of the elements heavier than iron, such as Gold, Europium, and Uranium. These elements are created in Type II supernovae and neutron star mergers [3],[4]. Both of these processes could not have occurred until after the initial enrichment by the earliest generation of

stars of elements through to iron.

Because of the unique paths these enrichment processes take, we can identify stars by the abundance of some of these s-process and r-process elements, such as Barium and Europium respectively. This allows us to identify different factors that went into the enrichment and formation of specific stars as well as allowing us to test our models for how these elements were created.

1.2 Metal-Poor Stars

Because of this growing enrichment over time, we can use metal-poor stars as an astronomical artifact of sorts. These metal poor stars are stars the we measure a metallicity of [Fe / H] ≤ -2.0 with [Fe / H] defined as,

$$[\text{Fe / H}] = \log_{10}\left(\frac{N_{\text{Fe}}}{N_{\text{H}}}\right)_{\text{Star}} - \log_{10}\left(\frac{N_{\text{Fe}}}{N_{\text{H}}}\right)_{\text{Sun}} \qquad \text{(Eq. 1)}$$

There is some debate as to what metallicities qualify as metal poor or very metal poor, but for the purposes of this paper we define the metallicities we are interested in at [Fe / H]≤ -2.0. These low metallicity stars allow us to extrapolate how the Milky Way has evolved chemically over time by analyzing a combination of their elemental abundances, alongside our understanding of stellar evolution. Most of these metal-poor stars have been found to have similar abundance patterns [5], [6]. Which tells us that they were likely formed around the same overall time as a population and that the enrichment in the majority of these stars is typical of that generation. This allows metal-poor stars to be useful in learning about what abundances would have been typical in the Milky Way at the time, and how chemical abundances in the Milky Way have evolved since the metal-poor stars' formation. There are, however, a significant number of metal-poor stars that have been found to exhibit peculiar chemical abundances, see [7] for further detail. Because of the uniformity of most metal-poor stars, the peculiarities in the abundances of elements for these stars must have been enriched from external interaction events. One trend that is interesting for this study is that as we decrease our metallicity, we find that there are greater enhancements in carbon [7]. Carbon is an element created in last stages of a star's lifespan, but the stars this has been observed in are on the main sequence and should not have begun to create carbon. This implies

that this enrichment in carbon comes from a separate interaction, that of an earlier generation of stars. This again allows this subset of metal poor stars to be of interest in understanding the earliest generation of stars from not only their low metallicity, but also their enhancements in carbon. A star exhibiting these characteristics is referred to as a Carbon Enhanced Metal Poor (CEMP) Star.

1.3 CEMP Stars

For a metal poor star to be considered Carbon Enhanced it needs to have a carbon abundance of [C / H] $\geq +0.7$ where the carbon abundance is similarly defined as in equation 1. Due to the logarithmic nature of this abundance fraction, this corresponds to having five times as much carbon as our Sun. Given that our sun has a higher overall metallicity than these metal poor stars, we would not expect that these metal poor stars have such great enrichment in carbon without there being an external interaction. This overabundance of carbon is believed to be a sort of residue left over from the Population III stars that directly preceded these CEMP stars. This makes CEMP stars even more useful in trying to understand Population III stars and galactic chemical evolution. However, not all CEMP stars had to gain this enhancement from Population III stars, they could have just as easily been enriched by younger stars that have since gone through their life cycle.

There are many subsets of CEMP stars, [8], but in this paper we will focus on just a few. CEMP stars that exhibit an abundance of s-process elements are referred to as CEMP-s stars [8]. They are believed to have gained this enrichment by siphoning the s-process elements off of an AGB companion star onto the CEMP star through mass transfer caused by Roche-lobe overflow as well as stellar wind [9]. Because of this, we find that CEMP-s stars are almost always in a binary system with an AGB star. We use Barium abundance to detect if a CEMP star does have s-process elements present as it is easy to detect in the stellar spectra. Similarly, CEMP stars that exhibit an abundance of r-process elements are referred to as CEMP-r stars [8]. These stars are not believed to have been enhanced from being in a binary system, but rather the r-process elements were already present in the gas cloud the CEMP-r star would form from. Many of these r-process elements would have been created in neutron star mergers alongside supernovae [3],[4]. We use Europium abundance to classify a CEMP-r star as it is the easiest r-process element to detect in

stellar spectra.

It is also possible for a CEMP star to exhibit abundances in s-process and r-process elements. These are known as CEMP-r/s stars. While it was initially thought that this abundance pattern could be a hybridization of the two previously outlined methods, studies by [10] have shown that the observed abundances do not line up properly with this, leading to the suggestion of an intermediate process. This intermediate process (i-process) is thought to lead to the synthesis of both s-process and r-process elements in the ratios observed. The mechanisms of such a process are currently not well understood, but is believed that the i-process would take place off of the CEMP-r/s star [11], which would imply that CEMP-r/s stars are in binary systems.

1.4 Binary Stars

Binary Stars are two gravitationally bound stars that orbit one another about a common barycenter. These systems can be detected in a multiple different ways; through analyzing the shifting of spectroscopic lines over time and photometric measurements to find eclipsing binaries are the two simplest. The spectroscopic measurements do require that the alignment of the system is such that we would observe radial motion of the stars in their orbits. The photometric measurements, however, require the system to be lined up such that we could see a dip in the primary star's brightness, and do so when we are observing it. Because of this, spectroscopic measurements are more reasonable to detect if a star is in a binary system. In this study, we will be using spectroscopically obtained radial velocities to determine if stars are in a binary system.

Stars that are in binary systems can have some mass transfer between the two stars. This can be caused by both interstellar winds and Roche-lobe overflow [9]. The two methods are determined by the orbital properties of the binary system. Systems that have distant orbits will exchange through interstellar winds, while closer orbits will allow for Roche-lobe overflow. This mass transfer can have serious effects on the orbital dynamics of the system [12].

Since the i-process is believed to take place off of CEMP-r/s stars, that would require for there to be some kind of mass transfer between the CEMP-r/s star and its companion. This is not explored in this paper, but will important in understanding the enrichment process of CEMP-r/s

stars. Before there is work on mass transfer and understanding the i-process, we can use radial velocity measurements to determine if CEMP-r/s stars are commonly in binary systems or not.

2. METHODS

In this study, I take data gathered by Dr. Terese T. Hansen over the past two years, reducing spectroscopic data she gathered at the McDonald Observatory. I combine this with publicly available literature data on these same stars and plot their radial velocities over time to check if they may be binaries.

2.1 Determining Radial Velocities of Target Stars

Radial velocities of the target stars are determine via cross-correlation of the extracted 1D spectra using the fxcorr task in IRAF. The fxcorr task performs a Fourier Cross-Correlation between the 1d spectra of a target star and a standard star.

This cross correlation can be described mathematically as follows [13],

let $f \star g$ denote the cross-correlation of f(t) and g(t).

$$f \star g = \int_{-\infty}^{\infty} \bar{f}(t) g(t+\tau) d\tau$$

$$= \int_{-\infty}^{\infty} \left[\int_{-\infty}^{\infty} \bar{F}(v) e^{2\pi i v \tau} dv \int_{-\infty}^{\infty} G(v') e^{-2\pi i v'(t+\tau)} dv' \right] d\tau$$

$$= \int_{-\infty}^{\infty} \int_{-\infty}^{\infty} \bar{F}(v) G(v') e^{-2\pi i v' t} \delta(v' - v) dv' dv$$

$$= \mathcal{F}\left[\bar{F}(v) G(v)\right]$$

thus,

$$f \star g = \mathcal{F}\left[\bar{F}(v) G(v)\right]$$

Where $\mathcal{F}$ denotes the Fourier transform of the argument and $\bar{F}(v)$ is its complex conjugate.

What this tells us is how similar two functions are to one another. Imagine two wave-forms f and g, $f \star g$ would look like sliding f along a rail next to g and plotting the amount of overlap between the two for each position along the rail. When we perform a cross-correlation on our data, we compare the lines of a target star to what's known as a radial velocity standard star. These

standard stars have well measured and constant radial velocities, and can be used as a benchmark to calibrate our data against. The cross-correlation will tell us how much our target star's spectrum is redshifted compared to the standard star, and what the corresponding radial velocity difference is.

For our radial velocity data, we also need to know how accurate our measurements are. One surprisingly useful feature of the spectra we will study is the interference from Earth's atmosphere. There are a set of lines known as the Telluric Lines which are caused by oxygen and water vapor in the Earth's atmosphere. By going through to check how much these lines have shifted compared to their nominal laboratory wavelengths, we were able to check how well calibrated the device used to gather the data was for each star in our set. This gave us a measure of the stability for every measurement we analyzed. To do this I went through and examined each star's spectrum and identified where each of the Telluric lines were located. I fed these into the IRAF task rvidlines which was also fed the nominal location of these lines. The task then measured the shifting of the lines from their nominal values and determined what the "radial velocity" of the measurement was. But, since these were the Telluric Lines we were measuring, that "radial velocity" is not real, and is our base error in any measurement. This gives us our baseline for how accurate we can be with any of our measurements before we do the cross correlation.

2.2 Creating Plots of Radial Velocity Change Over Time

The first step in identifying whether the star in question is a binary is to make a plot of the radial velocity over time. For this, I combine the new radial velocity solutions found from Dr. Terese T. Hansen's observations over the past two years with literature data about the same stars. For each star I plot the radial velocity and associated uncertainties on the y-axis and time on the x-axis. Along with this plot, we need to determine if these variations are significant when taking into account the error caused both by machine stability, and in the measurement itself, this will be done by analyzing the plots alongside measurements of redshift in the telluric lines of the spectrum. From this we will be able to make a rough estimate on the number of stars in our sample that could be binaries. We likely will not have enough data for any of these stars to conclusively

determine if they are in binary systems, but this will be a useful starting point for future research into CEMP-r/s stars.

2.3 Selection

The stars selected for this were determined based off their abundances from literature data. A table on the following page lists these for the stars we gathered data on. The criteria are based off a number of sources which have evolved from [8] with (0.0 < [Ba/Eu] < +0.5) and (-1.5 < [Sr/Ba] < -0.5) being the criteria we are interested in. These stars also had to be bright enough to be observed at the McDonald observatory throughout the year in a magnitude range of V = 8.4 to 16.5. Exposure times at one hour were sufficient to obtain a signal to noise ratio of around 10 for a V = 14 star on the McDonald Observatory's TS23 spectrometer and 2.7 m telescope.

Object	RA	DEC	V	[Fe/H]	[C/Fe]	[Ba/Fe]	[Eu/Fe]	Reference
CS31070-073	0:16:38	5:54:31	14.4	-2.55	1.34	2.28	2.74	Allen 2012
CS22183-015	2:28:22	3:01:15	13.17	-2.76	-2.81	1.97	1.58	Cohen 2013
2MASSJ01261795+0607248	1:55:55	6:49:53	15.7 (AB g)	-3.16	2.93	2.79		Aoki 2008
HE0143-0441	2:48:12	5:38:05	16.38	-2.36	2.19	2.32	1.5	Cohen 2013
HE0336+0113	3:46:49	1:37:38	14.96	-2.73	2.46	2.53	1.22	Cohen 2013
HE0414-0343	4:44:26	4:28:19	11.04	-2.24	1.44	1.87	1.23	Hollek 2015
SDSSJ071105.43+670228.2	7:20:02	67:49:05	16.1	-2.91	1.98	0.81		Aoki 2013
SDSSJ074104.22+670801.8	7:48:02	67:10:58	15.8 (AB g)	-2.87	0.74	0.27		Aoki 2013
SDSSJ091243.72+021623.7	10:24:52	2:55:32	15.37	-2.68	2.22	1.47	1.18	Behara 2010
2MASSJ09240185+4059288	9:27:05	41:03:48	15.7 (AB g)	-2.56	2.73	1.86		Aoki 2008
HE1029-0546	11:51:12	7:14:15	15.63	-3.28	2.64	0.8		Hansen 2015
HE1031-0020	11:14:21	0:49:58	14.3	-2.86	1.79	1.55	<0.86	Cohen 2013
BD-012582	12:55:12	3:01:13	9.6	-2.62	0.86	1.05	0.36	Roederer 2014
BS16077-077	12:22:36	28:22:14	12.32	-2.05	2.39	0.75	0.04	Allen 2012
HE1159-0525	12:06:29	5:41:54	15.3	-2.96	2.03	1.53	0.74	Cohen 2013
SDSSJ124502.68-073847.1	12:49:28	7:45:51	16.3 (AB g)	-3.16	2.53	2.08		Aoki 2013
SDSSJ134913.54-022942.8	14:11:34	3:40:18	16.6 (AB g)	-2.98	2.87	2.15	1.6	Behara 2010
HE1410-0004	14:20:44	1:12:16	15.49	-3.07	2.2	1.06		Cohen 2013
CS30301-015	16:42:44	3:01:03	13.04	-2.64	1.72	1.49	0.22	Aoki 2002
HE1509-0806	16:20:17	9:24:01	14.8	-2.91	2.19	1.93	<0.97	Cohen 2013
SDSSJ162603.61+145844.3	16:32:01	16:11:52	17.2 (AB g)	-2.99	2.86	1.69		Aoki 2013
2MASSJ17073392+5850598	18:03:33	60:29:31	16.1	-2.57	2.14	3.44		Aoki 2008
HD196944	21:56:48	8:11:25	8.4	-2.41	1.08	1.23	-0.11	Placco 2015
HE2150-0825	21:53:16	8:41:22	14.96	-1.98	1.31	1.65		Barklem 2005
HE2158-0348	23:06:38	3:54:07	15.71	-2.71	1.99	1.68	0.79	Cohen 2013
HE2232-0603	23:53:03	6:16:54	16.51	-2.28	1.35	1.3	0.47	Cohen 2013
HE2240-0412	24:18:48	4:01:41	15.81	-2.2	1.31	1.32		Barklem 2005
HE2251-0821	22:55:22	9:20:02	15.73	-2.96	1.97	1.75		Cohen 2013
CS22949-008	24:53:53	4:47:42	14.15	-2.45	1.93	0.77		Allen 2012
BS16080-175	16:52:28	57:12:28	14.35	-1.86	1.94	1.5	1.04	Allen 2012
BS17436-058	13:36:46	45:03:08	13.83	-1.09	1.71	1.68	1.28	Allen 2012
CS30338-089	23:23:21	10:19:26	14.14	-2.49	2.06	2.25		Aoki 2007
HE1405-0822	15:18:37	8:38:24	14	-2.37	1.9	1.92	1.52	Cui 2013
HKII17435-00532	11:49:33	117:04:57	13.15					

3. DATA REDUCTION

3.1 Data Reduction and Calibration

In order to obtain wavelength solutions from our spectroscopic data, the data needs to go through a series of steps known as data reduction. Using the image reduction software IRAF, a user can run through a series of steps to take the raw data from the echelle spectrograph and find what corresponds to different wavelengths allowing for identification of chemical abundances. These steps include removing bad pixels that did not function correctly on the imaging sensor that gathered the data, removing pixels that have been struck by a cosmic ray, and removing scattered light from sources other than the star being imaged. IRAF also allows a process called optimal extraction that takes the original data and restructures it, preserving the information encoded on the pixels, but optimizing the signal-to-noise ratio. After this, IRAF allows a user to create a wavelength scale by comparing the star's spectrum to a well known source, in our case we use a Thorium-Argon Lamp which is part of the instrument used to collect the data. Once this wavelength scale is found it can be utilized to find wavelength solutions. Finding the wavelength solution is the goal of data reduction for use later identifying features in a star's spectrum. These features will later allow us to find radial velocities of these stars. Since we will know which peaks in the wavelength solution occur in what location, we will be able to deduce radial velocity by the shift in these peaks' locations. This is due to the Doppler Shift, if a star is moving away from us we will see the wavelengths shifted slightly towards the red, while if it is moving towards us it will be shifted towards the blue. These shifts can be compared with a standard star that anchors radial velocities to determine the star in question's radial velocity. Going through the steps of spectroscopic reduction in more detail, the first task we will take on is the removing of bad pixels. We can go through our data and identify pixels that did not properly record any data. This is because they are somehow damaged on the CCD we are using to catch light on. We run a task in IRAF that removes and smooths over any pixel identified as bad in a text document we feed the task. This is done by taking the average of

the surrounding good pixels and replacing the bad value with that. The second task we take on in this process is calculating the median flat image. A flat is an image taken before observation of any targets that can be used to determine how the pixels react to uniform light. This allows for calibration of errors caused by pixel to pixel. The next task is to remove cosmic rays. Over the course of an exposure it is not uncommon to be bombarded with multiple cosmic rays, which will show up as bright lines across many different pixels. Similarly to the bad pixel corrections, this task will take the average of the surrounding pixels and replace the bad one. The difference being that in this case the task goes through pixel by pixel to identify which ones have been affected by cosmic rays. We do this by setting the amount of variance from mean any pixel can have before it gets flagged. The fourth task we will need to do is combining our science frames with each other. This is done through a weighted sum that favors longer exposure times, but can further get rid of any anomalies one of the exposures may have had.

3.2 Database, Optimal Extraction, and Final Corrections

Next we will create a reference id for all of the apertures. This is so we have a database to work against in the future. The sixth step we take in image reduction is removing the scattered light from the median flat we found earlier and the science frames. This utilizes the reference we just made. Next we will create a normalized flat. This is done by dividing the original composite flat by the new smooth flat. Following this we will still need to do what's called flat correcting. To do this we input to the task both our science and normalized flat images. The output will correct any inconsistencies that the flat found with the CCD. After this we perform a task called optimal extraction. This process takes our 2D image that needs processing and pulls all the data in one line together into one pixel. Following this we will once again remove cosmic rays. In the event that any cosmic rays somehow avoided getting smoother, or weren't properly smoothed over, this will catch them and again take the average of the surrounding pixels.

3.3 Finding Wavelength Solutions

For our penultimate step we will generate the wavelength scale we are going to be fitting all of this newly compacted data to. To do this we are going to open the spectra of a Thorium-Argon

Frame, which is the result of shining a specific lamp onto the spectrograph before the observations This lamp has a well defined spectrum and we will use it to create a scale against which we will later use to find wavelength solutions for all of our input science spectra. Lastly in this data reduction process we are going to go though each of the optimized spectra for the science frames. To do this we use refspec to compare and match the spectra to the reference spectrum we just generated. Once this has happened, the spectrum will have wavelengths matching to its spectral features, and will allow me to identify how much they've been shifted due to their orbits.

4. RESULTS

The results of our radial velocity observations at the McDonald Observatory of CEMP-r/s stars will be reported on in this chapter. Along with the measured data, there is some literature data included for the stars as well. This will go over the mean heliocentric radial velocities found in our cross-correlation, their standard deviations, number of orders in the spectra used to compute this radial velocity, and Modified Julian Date. The literature data does not always include errors in measurement, while the error in measurements of this study are the standard deviations of the cross-correlation.

The results, which will be shown on the next few pages, suggest that CEMP-r/s stars have a high fraction that are a part of binary systems. Of our set, 21 have enough measurements to begin to see if there is a large enough dispersion in the heliocentric radial velocities to begin to determine if the star is in a binary system. Of these 21 stars, an optimistic count of 18 appear to be potential binaries and a pessimistic count of 11. This strongly suggests, if follow up studies confirm this, that CEMP-r/s stars gain their enrichment through mass transfer from binary partners. One thing to keep in mind which is not shown in the following tables or plots is the underlying stability of the device. From checking the shifting of the Telluric Lines in each stellar spectra, we were able to determine how much this may be an issue. We found that the measuring device was stable to with 1 km/s for the measurements present so it should not cause major errors to the data when compared to the standard deviation of the cross-correlation.

4.1 Resulting Tables

Tables listing the mean heliocentric radial velocity, standard deviation, number of orders used, and modified Julian date for each star is provided in this section.

	Mean Heliocentric Radial Velocity	Standard Deviation	Number of Orders	MJD
CS30338-089	-132.92	10.90	28	58701
	-118.52	2.01	26	59051
	-121.97	2.28	26	58802
HD196944	-174.42	1.10	37	58701
	-173.06	0.86	36	58686
	-169.01	1.18	37	59051
	-173.21	1.21	41	58802
	-173.04	1.07	42	58739
HE2158-0348	60.12	1.78	13	58701
HE2158-0348	60.12	1.78	13	58701
J17073392	-92.54	27.34	4	58701
	-92.04	0.96	47	59051
2MASSJ01261	-43.72	3.60	14	58831
CS22183-015	-71.95	1.75	24	58831
CS22949-008	-156.05	1.72	16	58831
	-156.68	4.62	11	58802
HE0414-0343	15.67	1.83	46	58831
	17.55	3.23	60	58739
	5.28	2.36	59	59113
HE1031-0020	63.94	3.19	13	58831
	64.62	2.36	23	59210
	64.25	0.49	3	58888
	62.41	2.26	26	58940
	61.38	2.79	27	58963

	Mean Heliocentric Radial Velocity	Standard Deviation	Number of Orders	MJD
BS16077-077	66.54	1.03	39	59210
	64.15	1.24	37	5862
	64.31	2.38	6	58888
	64.68	1.44	39	28941
	62.49	1.28	38	58966
BD-012582	1.45	1.46	58	58888
	0.46	1.15	43	58622
HE1305+0007	224.88	2.50	37	58888
	228.45	1.77	35	58940
	226.05	2.13	35	58964
HKII17435	32.21	2.28	27	58888
	34.66	0.91	43	58622
	35.31	1.43	42	58940
	33.65	1.38	43	58966
BS16080-175	-255.71	1.35	19	59051
	-256.22	1.06	31	58622
	-255.55	2.83	16	28686
	-257.66	1.15	37	58938
	-257.13	1.31	38	58964
HE1159-0525	29.17	0.90	48	58622
	70.99	2.61	27	58965
HE1405-0822	119.12	4.72	3	58888
	120.20	1.42	36	58939
	116.82	1.50	29	58965
SDSSJ071105	-22.79	0.62	47	58802

	Mean Heliocentric Radial Velocity	Standard Deviation	Number of Orders	MJD
HE2150	-73.89	1.87	17	59051
	1.21	1.61	45	58802
CS31070-073	-141.98	10.03	9	58802
	-126.03	2.78	17	59113
HE0336+0113	59.73	1.87	16	59113
HE0143	121.14	33.11	4	58831
BS17436-058	14.43	1.57	38	58622
	14.94	1.65	39	58941
	13.00	1.07	43	58965

4.2 Radial Velocity Plots

The following are plots of CEMP-r/s stars that exhibit enough variance in the heliocentric radial velocities that they may be in binary systems. These plots have a common coloring system, points that are blue are from literature sources which will be listed, and points that are black are from the data gathered for this study.

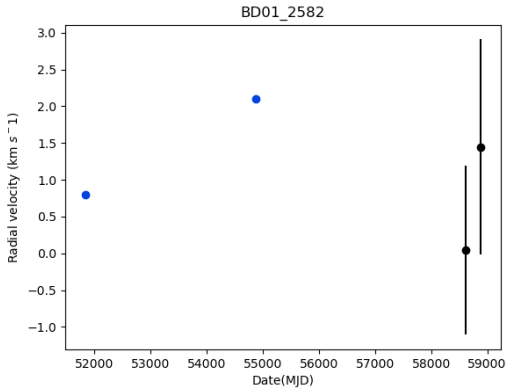

(a) Literature data includes: [14][15]

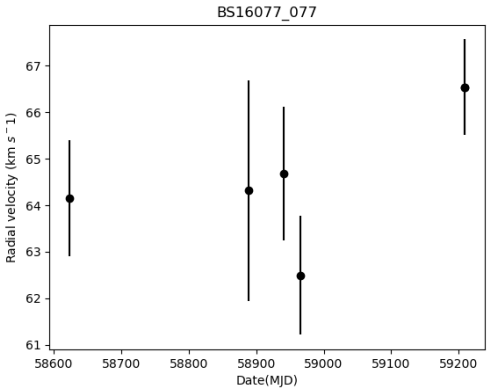

(b)

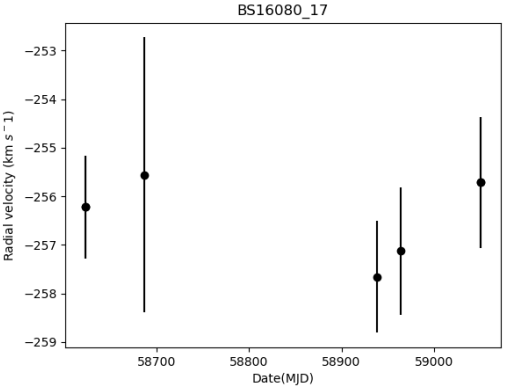

(c)

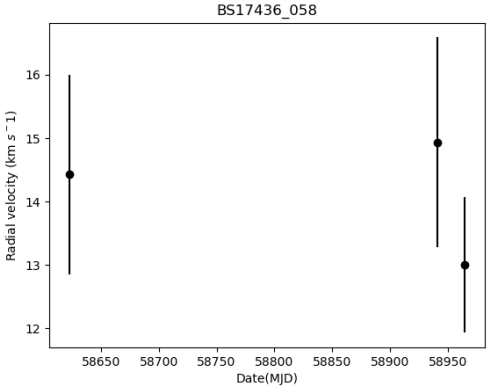

(d)

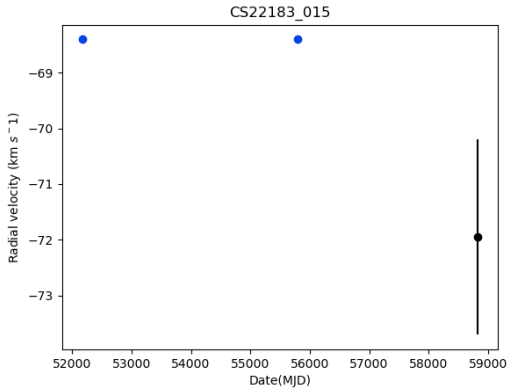

(a) Literature data includes:[16]

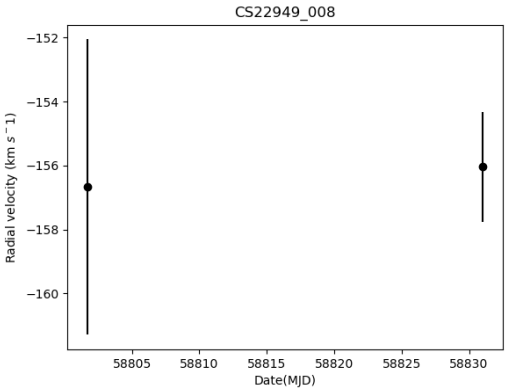

(b) [17] believes this is a double lines binary.

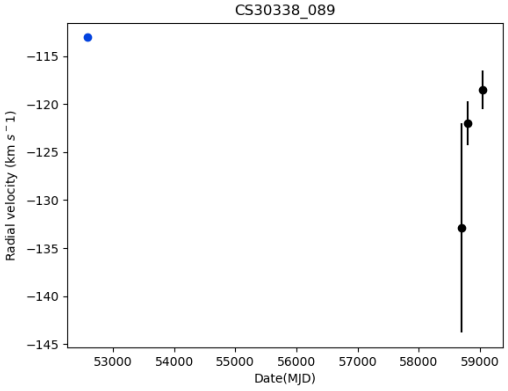

(c) Literature data includes: [18]

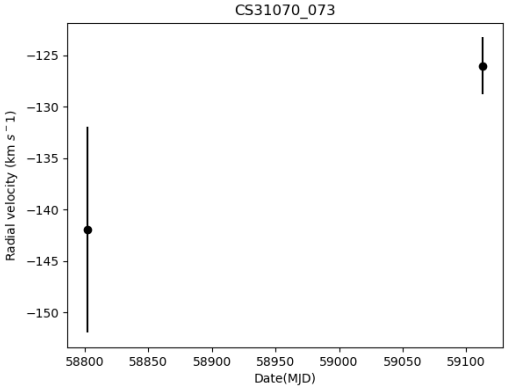

(d)

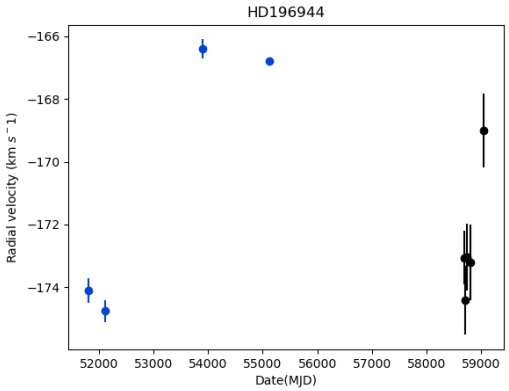

(a) Literature data includes: [19], [20], [21], [22]

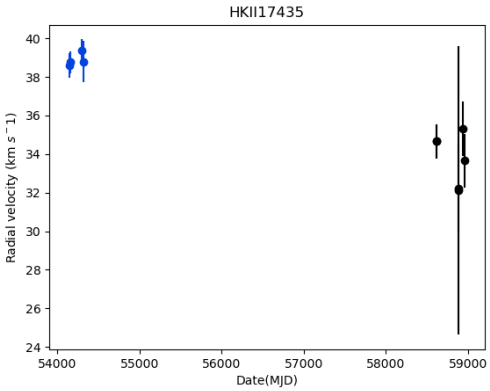

(b) Literature data includes: [23]

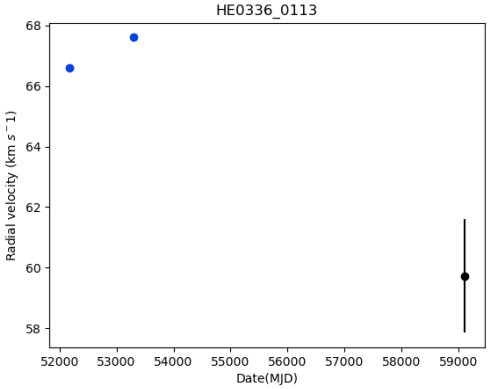

(c) Literature data includes: [16]

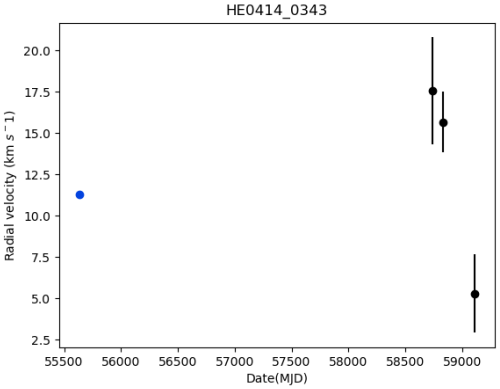

(d) Literature data includes: [24]

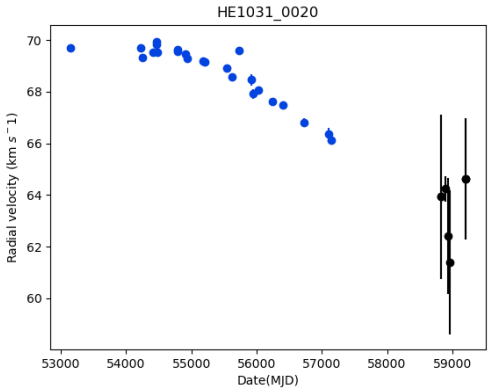

(a) Literature data includes: [16] [25]

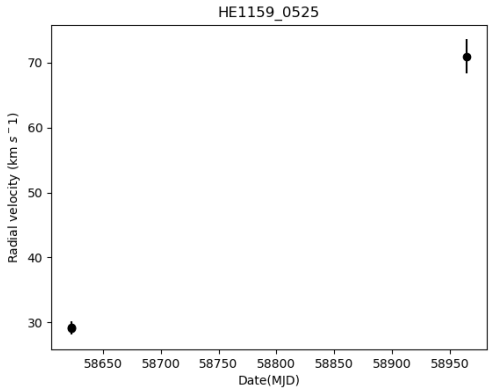

(b)

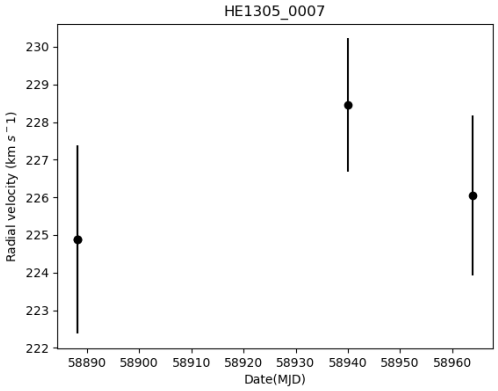

(c)

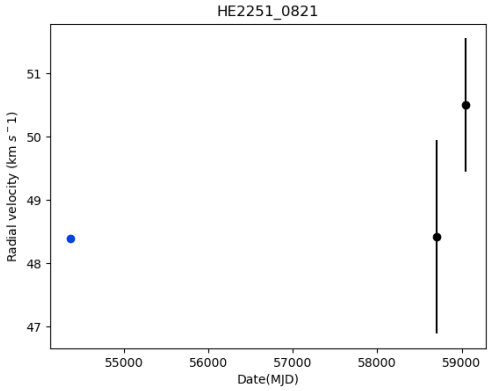

(d) Literature data includes: [16]

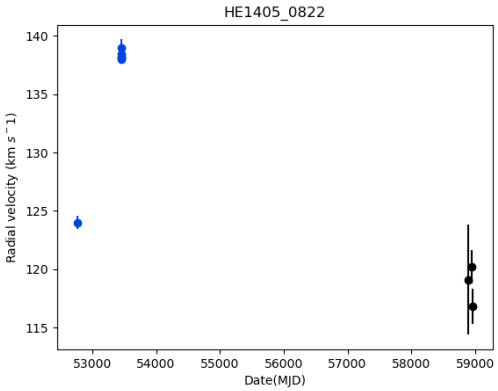

(a) Literature data includes: [26]

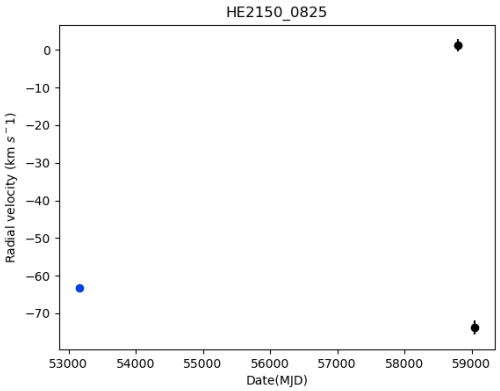

(b) Literature data includes: [27]

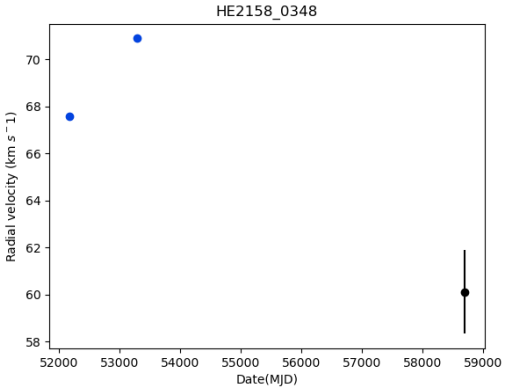

(c) Literature data includes: [16]

5. DISCUSSION

The results of this study suggest that many of these CEMP-r/s stars could be part of binary systems. The most optimistic estimate of the binary fraction of these stars would be $\approx 85.7\%$. We will further discuss the implications of this and why some of the stars do not currently give results consistent with being in a binary system.

5.1 Implications

If CEMP-r/s stars do gain their enrichment through binary mass transfer, that will give future studies a place to start on determining what the method is that gives CEMP-r/s stars their peculiar abundances. It would also suggest that CEMP-r/s stars are likely not useful in determining features about Population III stars, as they have been contaminated by their binary partner star and would not give a pure representation of the elemental abundances created in the deaths of Population III stars. Because of this, CEMP-r/s stars would need to be sorted out from typical Metal-Poor stars for studies on the relation between Metal-Poor stars and Population III stars. Future studies on the enrichment of CEMP-r/s stars also will be able to focus on what the binary partners may be that would allow for the synthesis of both s-process elements and r-process elements in the ratios observed as discussed in the introduction. Whether there is or is not an i-process that creates these peculiar chemical abundances is not in the scope of this study, but hopefully it can lend some guidance to future projects that begin to uncover this.

5.2 Error Sources

Some of the stars in the sample did not appear to be in binary systems based off the data gathered, but given the high fraction of CEMP-r/s stars that are in binary systems these apparent non-binaries may very well be illusory. There are a number of issues that may cause us not to be able to detect if a star is in a binary system. The amplitude of radial velocity shift may be low enough that it is within our margins of error, or the shifts in the spectroscopic data may be so small that our resolution is not high enough to detect them. It is also distinctly possible, given the limited

number of observations, that the orbital periods of these stars may be greater than the length we observed them. We may even have gotten unlucky and observed a star at the same point in its orbit. There are also a number of stars that only have one measurement, and literature data that is not focused on radial velocities may not always be as reliable as studies that are focused on obtaining radial velocities.

6. CONCLUSION

The use of low metallicity stars to probe the chemical evolution of the Milky Way is exciting, but as we have seen, a large fraction of low metallicity stars show large enhancements in carbon. As discussed in the introduction, the lower in metallicity you search, the larger this fraction of carbon enhanced stars becomes. This make CEMP stars an important subset of metal-poor stars that show peculiarities in the otherwise uniform abundances in metal-poor stars. Understanding these CEMP stars better will allow for a better understanding of both the chemical history of the Milky Way and earliest generation of stars. In this study, we focused on CEMP-r/s stars and explored how they may gain their peculiar abundances in binary systems. The heart of this study was in the reducing of spectroscopic data and extracting radial velocities from the spectra using data gathered at McDonald Observatory and including previous studies' radial velocity data. From this, we were able to find that it appears as many as 85.7% of the observed CEMP-r/s stars may be in binary systems, and there are a number of contributing factors that could lead to this binary fraction being higher. Of these, the leading contributors of this are likely the limited time range of the data gathering period alongside a limited number of observations for each star. This implies that CEMP-r/s stars gain their peculiar abundances through mass transfer with their binary partners and are likely too contaminated to be used as a cosmic "relic" to better understand the chemistry of the earliest stars in the Milky Way. Nonetheless, the enrichment of CEMP-r/s stars is still an open question, but the results of this paper support the idea that binary partners play a role in the peculiar abundance pattern observed in these stars.

REFERENCES

[1] A. Heger and S. E. Woosley, "The Nucleosynthetic Signature of Population III," , vol. 567, pp. 532–543, Mar. 2002.

[2] R. Gallino, C. Arlandini, M. Busso, M. Lugaro, C. Travaglio, O. Straniero, A. Chieffi, and M. Limongi, "Evolution and Nucleosynthesis in Low-Mass Asymptotic Giant Branch Stars. II. Neutron Capture and the S-Process," , vol. 497, pp. 388–403, Apr. 1998.

[3] E. M. Burbidge, G. R. Burbidge, W. A. Fowler, and F. Hoyle, "Synthesis of the Elements in Stars," *Reviews of Modern Physics*, vol. 29, pp. 547–650, Jan. 1957.

[4] E. Ramirez-Ruiz, M. Trenti, M. MacLeod, L. F. Roberts, W. H. Lee, and M. I. Saladino-Rosas, "Compact Stellar Binary Assembly in the First Nuclear Star Clusters and r-process Synthesis in the Early Universe," , vol. 802, p. L22, Apr. 2015.

[5] R. Cayrel, E. Depagne, M. Spite, V. Hill, F. Spite, P. François, B. Plez, T. Beers, F. Primas, J. Andersen, B. Barbuy, P. Bonifacio, P. Molaro, and B. Nordström, "First stars V - Abundance patterns from C to Zn and supernova yields in the early Galaxy," , vol. 416, pp. 1117–1138, Mar. 2004.

[6] W. Aoki, T. C. Beers, Y. S. Lee, S. Honda, H. Ito, M. Takada-Hidai, A. Frebel, T. Suda, M. Y. Fujimoto, D. Carollo, and T. Sivarani, "High-resolution Spectroscopy of Extremely Metal-poor Stars from SDSS/SEGUE. I. Atmospheric Parameters and Chemical Compositions," , vol. 145, p. 13, Jan. 2013.

[7] V. M. Placco, A. Frebel, T. C. Beers, and R. J. Stancliffe, "Carbon-enhanced Metal-poor Star Frequencies in the Galaxy: Corrections for the Effect of Evolutionary Status on Carbon Abundances," , vol. 797, p. 21, Dec. 2014.

[8] T. C. Beers and N. Christlieb, "The Discovery and Analysis of Very Metal-Poor Stars in the Galaxy," , vol. 43, pp. 531–580, Sept. 2005.

[9] C. Abate, O. R. Pols, R. G. Izzard, S. S. Mohamed, and S. E. de Mink, "Wind Roche-lobe overflow: Application to carbon-enhanced metal-poor stars," , vol. 552, p. A26, Apr. 2013.

[10] M. Lugaro, A. I. Karakas, R. J. Stancliffe, and C. Rijs, "The s-process in Asymptotic Giant Branch Stars of Low Metallicity and the Composition of Carbon-enhanced Metal-poor Stars," , vol. 747, p. 2, Mar. 2012.

[11] M. Hampel, R. J. Stancliffe, M. Lugaro, and B. S. Meyer, "The Intermediate Neutron-capture Process and Carbon-enhanced Metal-poor Stars," , vol. 831, p. 171, Nov. 2016.

[12] M. I. Saladino, O. R. Pols, E. van der Helm, I. Pelupessy, and S. Portegies Zwart, "Gone with the wind: the impact of wind mass transfer on the orbital evolution of AGB binary systems," , vol. 618, p. A50, Oct. 2018.

[13] E. W. Weisstein, "Cross-correlation theorem."

[14] G. R. Ruchti, J. P. Fulbright, R. F. G. Wyse, G. F. Gilmore, O. Bienaymé, J. Bland-Hawthorn, B. K. Gibson, E. K. Grebel, A. Helmi, U. Munari, J. F. Navarro, Q. A. Parker, W. Reid, G. M. Seabroke, A. Siebert, A. Siviero, M. Steinmetz, F. G. Watson, M. Williams, and T. Zwitter, "Observational Properties of the Metal-poor Thick Disk of the Milky Way and Insights into its Origins," , vol. 737, p. 9, Aug. 2011.

[15] A. E. García Pérez and F. Primas, "Li and Be depletion in metal-poor subgiants," , vol. 447, pp. 299–310, Feb. 2006.

[16] J. G. Cohen, N. Christlieb, I. Thompson, A. McWilliam, S. Shectman, D. Reimers, L. Wisotzki, and E. Kirby, "Normal and Outlying Populations of the Milky Way Stellar Halo at [Fe/H] <-2," , vol. 778, p. 56, Nov. 2013.

[17] T. Masseron, J. A. Johnson, S. Lucatello, A. Karakas, B. Plez, T. C. Beers, and N. Christlieb, "Lithium Abundances in Carbon-enhanced Metal-poor Stars," , vol. 751, p. 14, May 2012.

[18] W. Aoki, T. C. Beers, N. Christlieb, J. E. Norris, S. G. Ryan, and S. Tsangarides, "Carbon-enhanced Metal-poor Stars. I. Chemical Compositions of 26 Stars," , vol. 655, pp. 492–521, Jan. 2007.

[19] S. Van Eck, S. Goriely, A. Jorissen, and B. Plez, "More lead stars," , vol. 404, pp. 291–299, June 2003.

[20] W. Aoki, S. G. Ryan, J. E. Norris, T. C. Beers, H. Ando, and S. Tsangarides, "A Subaru/High Dispersion Spectrograph Study of Lead (Pb) Abundances in Eight s-Process Element-rich, Metal-poor Stars," , vol. 580, pp. 1149–1158, Dec. 2002.

[21] I. U. Roederer, G. W. Preston, I. B. Thompson, S. A. Shectman, C. Sneden, G. S. Burley, and D. D. Kelson, "A Search for Stars of Very Low Metal Abundance. VI. Detailed Abundances of 313 Metal-poor Stars," , vol. 147, p. 136, June 2014.

[22] I. U. Roederer, J. E. Lawler, C. Sneden, J. J. Cowan, J. S. Sobeck, and C. A. Pilachowski, "Europium, Samarium, and Neodymium Isotopic Fractions in Metal-Poor Stars," , vol. 675, pp. 723–745, Mar. 2008.

[23] I. U. Roederer, A. Frebel, M. D. Shetrone, C. Allende Prieto, J. Rhee, R. Gallino, S. Bisterzo, C. Sneden, T. C. Beers, and J. J. Cowan, "The Hobby-Eberly Telescope Chemical Abundances of Stars in the Halo (CASH) Project. I. The Lithium-, s-, and r-enhanced Metal-poor Giant HKII 17435-00532," , vol. 679, pp. 1549–1565, June 2008.

[24] J. K. Hollek, A. Frebel, V. M. Placco, A. I. Karakas, M. Shetrone, C. Sneden, and N. Christlieb, "The Chemical Abundances of Stars in the Halo (CASH) Project. III. A New Classification Scheme for Carbon-enhanced Metal-poor Stars with s-process Element Enhancement," , vol. 814, p. 121, Dec. 2015.

[25] T. T. Hansen, J. Andersen, B. Nordström, T. C. Beers, V. M. Placco, J. Yoon, and L. A. Buchhave, "The role of binaries in the enrichment of the early Galactic halo. III. Carbon-enhanced metal-poor stars - CEMP-s stars," , vol. 588, p. A3, Apr. 2016.

[26] W. Cui, J. Shi, Y. Geng, C. Zhang, X. Meng, L. Shao, and B. Zhang, "The study of s-process nucleosynthesis based on barium stars, CEMP-s and CEMP-r/s stars," , vol. 346, pp. 477–492, Aug. 2013.

[27] P. S. Barklem, N. Christlieb, T. C. Beers, V. Hill, M. S. Bessell, J. Holmberg, B. Marsteller, S. Rossi, F. J. Zickgraf, and D. Reimers, "The Hamburg/ESO R-process enhanced star survey (HERES). II. Spectroscopic analysis of the survey sample," , vol. 439, pp. 129–151, Aug. 2005.